

Full-potential KKR calculations for MgO and divalent impurities in MgOA. N. Baranov,^{1,3,4} V. S. Stepanyuk,^{2,3,*} W. Hergert,³ A. A. Katsnelson,⁴ A. Settels,¹ R. Zeller,¹ and P. H. Dederichs¹¹*Institut für Festkörperforschung, Forschungszentrum Jülich, D-52425 Jülich, Germany*²*Max-Planck-Institut für Mikrostrukturphysik, Weinberg 2, 06120 Halle, Germany*³*Fachbereich Physik, Martin-Luther-Universität, Halle-Wittenberg, Friedemann-Bach-Platz 6, D-06099 Halle, Germany*⁴*Solid State Physics Department, Moscow State University, 119899 Moscow, Russia*

(Received 10 April 2000; revised manuscript received 08 May 2001; published 28 October 2002)

We present a detailed investigation of bulk properties of MgO and lattice relaxations around divalent impurities in MgO by means of the full-potential Korringa-Kohn-Rostoker Green's function method. The local-density approximation and the perturbative generalized gradient corrections are used to calculate the lattice constant and bulk modulus of MgO. We obtain a very good description of the ground properties of MgO. Lattice relaxations around divalent impurities in MgO are determined using an ionic version of the Hellmann-Feynman theorem.

DOI: 10.1103/PhysRevB.66.155117

PACS number(s): 71.20.-b, 71.15.Mb, 73.20.At

The ceramic oxide MgO has long been of interest as the prototype for simple oxides. Such characteristics of MgO as the high resistance to radiation, the transparency in the infrared and visible regions of the spectrum, and the mechanical strength open a wide perspective for many applications. MgO is a commonly employed substrate for epitaxial growth of multilayers and clusters.¹ It is also interesting to note that MgO is likely to be a major constituent of the Earth's lower mantle.

Despite the fact that MgO can be considered as a textbook example of an ionic system, its electronic structure,²⁻⁸ charge distribution,²⁻⁴ and physical properties⁹⁻¹⁸ are still under discussions. While there is no doubt that MgO must be regarded as highly ionic, the extent of covalent mixing is unclear. The most recent experiments² performed by the convergent beam electron-diffraction technique allowed to achieve a tenfold improvement in the accuracy in the measurements of structural factors for MgO. These experiments have revealed a small nonspherical distortion in the charge densities on the Mg and O ions. For oxygen the charge is distorted towards the Mg atom and for Mg the charge is pushed away from O.

Considering the various calculations for the lattice constant and bulk moduli of MgO,^{10,13,15,16,18-20} one can find that all methods give close results for the lattice constant, while there are discrepancies in results for bulk moduli. As an example we show in Table I results obtained by linear muffin-tin orbital (LMTO), linear augmented plane wave (LAPW), and pseudopotentials methods.

The main goal of this paper is to present ab initio studies of electronic structure and structural relaxations of MgO with divalent impurities (Be, Ca, and Sr). We perform self-consistent calculations of the forces and relaxations in these systems using the full potential Korringa-Kohn-Rostoker (KKR) Green's function method, which allows us to treat impurities in the infinite crystal. The effect of the structural relaxation on the charge distribution is demonstrated. To our best knowledge, there were only calculations of relaxations near impurities in ionic crystal using various cluster models. We choose divalent impurities for our studies because there is the considerable experimental and theoretical interest to structural changes in MgO caused, for example by Ca impurities.^{21,22} Presumably, the lattice strain induced by Ca ions in MgO leads to the surface segregation of Ca

TABLE I. Lattice constant and bulk modulus of MgO.

a (a.u.)	B_0 (Mbar)	
7.968, (Ref. 14)	7.732 (Ref. 17)	2.16, (Ref. 14) 1.71 (Ref. 17)
7.877, (Ref. 11)	7.917 (Ref. 19)	1.72, (Ref. 11) 1.72 (Ref. 19)
7.870, (Ref. 15)	7.922 (Ref. 13)	1.62, (Ref. 15) 1.46 (Ref. 13)
7.882, (Ref. 9)	7.97 (Ref. 20)	1.54, (Ref. 9) 1.61 (Ref. 20)
		Present work
7.855		1.697
8.028		1.533
7.956		1.721
8.126		1.538
		Experiment
7.958 (Ref. 33)		1.77 (Ref. 29)
7.953 (Ref. 34)		1.64 (Ref. 30)
7.970 (Ref. 35)		1.62 (Ref. 31)
7.921 (Ref. 36)		1.78 (Ref. 32)
		LMTO, LDA
		LAPW, (Ref. 11) FLAPW (Ref. 19) LDA
		Pseudopotentials, LDA
		GGA
		ASA LDA
		ASA-GGA
		FP LDA
		FP-GGA

impurities.²² Also, it was shown that Ca impurities induce structural transformations in MgO grain boundaries.²¹

Before attempting calculations on defects, we make extensive studies of the lattice constant and bulk moduli of MgO using the state of the art computational methods. Both the local-density and the general gradient approximations are used.

We describe the method only briefly, as it is the same as the one used in the previous work.^{23,24} Our calculations are based on density-functional theory in the local-density approximation (LDA) and the generalized gradient approximation (PW91-GGA).²⁵ We apply the multiple scattering KKR Green's function method. To solve the Kohn-Sham equations in the full-potential (FP) case the method developed by Dritler *et al.*²⁶ is used. In this method, the solution for the radial symmetric potential is calculated first, then the Born series is used to iteratively include the effect of the anisotropic part of the potential. The maximum angular momentum used in the expansion of the wave functions and the Green's function is set to $l_{max}=4$. The potential and the electron-density expansion include all angular momentum coefficients up to $2l_{max}=8$. In order to improve the space filling of the NaCl lattice (0.52), we introduce additional empty cells on the octahedral position, thus enhancing the space filling to the value of the bcc lattice (0.68), which improves the l convergence. The exact form of the resulting Wigner-Seitz cell is described by shape functions.²⁶ The electron density is calculated by a contour integral in the complex energy plane. The contour integral is evaluated with 114 complex energy points, which are chosen such that they include both the valence states and the semicore states of Mg, Ca, and Sr. Thus $2p^6$ states of Mg, $3s^2 3p^6$ states of Ca, and $4s^2 4p^6$ states of Sr are treated as valence states. For the bulk calculation the Brillouin-zone integrations are performed using 146 k points.

A perturbative treatment of gradient corrections is used. It has been recently demonstrated²³ that the GGA total energies can be evaluated with the self-consistent LDA densities as input. Very accurate lattice constants and bulk moduli of metal and semiconductors have been obtained in this approximation.

We also present in this paper results obtained in the atomic sphere approximation (ASA) for the potential, which, however, include the full charge density generated from the spherical potential.

In calculations of divalent impurities in MgO, the perturbed region around the defect is exactly embedded in the unperturbed crystal MgO by using a Green's function technique. A cluster of 77 perturbed potentials with T_d symmetry is used in our calculations. The equilibrium positions of the nearest-neighbor (nn) oxygen and the next nn magnesium atoms near the impurity are determined by the condition of vanishing forces. The forces are calculated using an ionic version of the Hellmann-Feynman theorem.²⁴ Since the positions in the perturbed crystal differ from the ones in the ideal host the corresponding host Green's function, the potentials, and the shape function are transformed to the new shifted positions as described in (Ref. 27).

First we present the results of our calculations for the perfect magnesium oxide crystal. The structural properties of

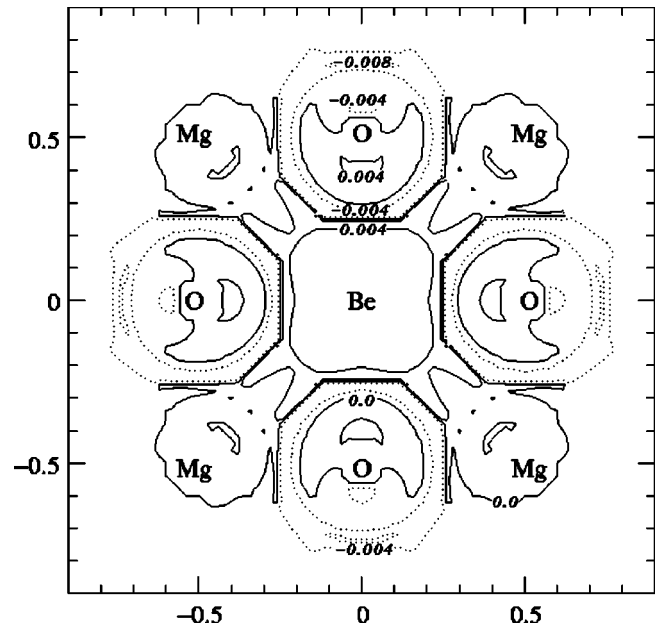


FIG. 1. Charge-density difference of relaxed and unrelaxed cluster of MgO+Be. Solid lines corresponds to positive values and broken lines to negative one. The contour intervals are $0.004 e/\text{Bohr}^3$.

MgO are determined by finding the minimum of the total energy as a function of the lattice constant. We use four approaches: FP-LDA, FP-GGA, ASA-LDA, and ASA-GGA. In ASA approximation for the potential the full charge density is used. The bulk modulus and the equilibrium lattice constant are determined using the equation of state proposed by Birch.²⁸ One should note that the bulk modulus is more sensitive to the calculated points chosen for the fit to the equation of state than the lattice constant.

Table I shows our results together with calculations performed by other groups and experimental data. One can see that the FP-LDA approach gives an excellent agreement with experiments for the equilibrium lattice constant and rather good result for bulk modulus. The effect of gradient corrections is well seen: GGA increases the lattice constant a and decreases bulk modulus B . The increase of the lattice constant may be explained by noting that the PW91-GGA functional favors electron-density inhomogeneties. In both the LDA and GGA approximations the lattice constant and bulk modulus are slightly larger in FP calculations, but the difference between FP and ASA results is rather small. The empty spheres introduced into the rocksalt structure of MgO improve the representation of the potential in ASA approach.

Comparing the present results with other calculations (cf. Table I) one can see that our method in FP LDA approach allows one to obtain a very good agreement with experimental data for both the lattice constant and bulk modulus and the most recent full-potential linear augmented plane wave (FLAPW) calculations of Bihlmayer and Blügel.¹⁹ It is necessary to note that precise measurements of bulk moduli are difficult, therefore experimental bulk moduli agree only within about 10%. Since the LDA approach gives slightly better results for the lattice constant, this approximation is also used for the impurity calculations in the following section.

TABLE II. Forces on Mg and O ions for different displacement [all forces are in $mRy/a(\text{Bohr})$]. The relaxations are given in percentages of the ideal Mg-O distance, i.e., of $a/2$, where a is the lattice constant.

System	O (% of relaxation)	Mg (% of relaxation)	O (Forces) [$mRy/a(\text{Bohr})$]	Mg (Forces) [$mRy/a(\text{Bohr})$]	Relaxation energy (eV)
MgO+Be	0.0	0.0	34.2	4.6	0.38
	-3.4	-0.8	0.65	-0.35	
MgO+Ca	0.0	0.0	-72.0	-4.2	0.44
	1.0	0.0	-52.2	-5.0	
	2.0	0.0	-32.7	-6.2	
	3.0	0.0	-13.2	-7.4	
	3.8	0.5	-0.08	-0.27	
MgO+Sr	0.0	0.0	-134.0	-15.4	1.76
	7.1	1.1	-0.45	-0.39	

Now we turn to the results on lattice relaxations around divalent impurities in MgO. First we present our results for a single Ca impurity, which substitutes an Mg atom. We neglect the distortion of distant neighbors and consider only the relaxation of the first (O) and the second (Mg) neighbors of the impurity. In Table II we present Hellmann-Feynman forces exerted on Mg and O for different displacements of Mg and O ions. It is seen that in the unrelaxed geometry the force acting on O is very large due to the difference in atomic sizes of Ca and Mg (the ionic radius of Ca is about 1.5 times larger than that of the Mg ion). Thus, Ca impurities introduce a large stress in MgO. Experimental studies on this system^{21,22} revealed that Ca ions segregate and concentrate in the outmost layer. It was suggested²² that the substitution of Ca for Mg in bulk site causes a large strain. Therefore, the surface segregation occurs to buffer it. Our results support such a scenario of segregation.

The relaxed atomic positions correspond to an outward relaxation of Mg and O around Ca impurity. We find that the displacements of O by 3.8% and Mg by 0.5% correspond to the equilibrium configuration, since in these relaxed positions the remaining forces are negligibly small.

Let us consider results for Be and Sr impurities in MgO. The size of Be cation is about two times smaller than the size of Mg cation. Also the wave functions of Be are more localized than the wave functions of Mg. Therefore, the interaction of Be impurity with O and Mg ions in unrelaxed geometry is expected to be relatively weak. Table II shows that the force acting on the O ions in MgO+Be is considerably smaller than the one in MgO+Ca and has an opposite direction. Thus, the Be impurity introduces a strong local tensile strain in MgO. The relaxed atomic positions in MgO+Be correspond to an inward relaxation of Mg and O around Be, i.e., relaxations are in the opposite direction to those for the Ca substitution, but the magnitude of the relaxations are similar, although the magnitudes of forces on the oxygen in the unrelaxed configurations differ by a factor of 2.

Compared to Be and Ca ions, the wave functions of Sr are more extended, which should lead to a stronger electronic rebonding in MgO+Sr compared to MgO+Ca. Also due to size arguments for Sr and Ca (difference in ionic radii is about 14%) one can expect that outward relaxations of Mg and O ions in MgO+Sr will be larger than in MgO+Ca.

Our results show (Table II) that the size effect and electronic rebonding lead to a drastic influence on atomic relaxations in MgO+Sr. We have found that the atomic displacements around the Sr impurity are about two times larger than for the Ca impurity (cf. Table II) and the relaxation energy is four times as large.

We want to briefly comment on the effect of the size of the perturbed region around the defect on relaxations. One can expect that such effect is most important for Sr impurity in MgO. Our calculations for a cluster of 113 perturbed atoms have shown that the displacements of the nn oxygen (7.2%) and the next nn magnesium atoms (1.7%) near Sr are close to results obtained for the cluster of 77 atoms (Table II). We have also checked the relaxation of several shells around Sr impurity and we have found that the relaxations are actually limited to the nearest O and Mg atoms. For example, the displacements of the third oxygen and the fourth magnesium atoms near Sr are only 0.1% and 0.6%.

Finally, we demonstrate the effect of lattice relaxations on the charge distribution around divalent impurities in MgO. The response of the charge density to the relaxations is studied by subtracting the charge density in unrelaxed system from that in the relaxed one. As an example, results for Be impurity in MgO are shown in Fig. 1. We found that the charge transfer during relaxations occurs between Mg and Be atoms, and empty cells on the octahedral positions. Inhomogeneous distribution of electronic density is well seen in Fig. 1.

In summary, we have shown that the FP KKR Green's function method allows us to obtain a very good description of the ground-state properties of MgO. We have performed ab initio calculations of forces and lattice relaxations in MgO with divalent impurities. Our results show that the atomic displacements in MgO with divalent impurities are determined by size effects and electronic rebonding around impurities.

The computations were performed on Cray computers of the Forschungszentrum Jülich and the German Supercomputer Center (HLRZ). Support of the Deutsche Forschungsgemeinschaft (DFG) through the SFB341 (Köln-Aachen-Jülich), Landes-Projekt Sachsen-Anhalt, and Deutscher Akademischer Austauschdienst (DAAD) are gratefully acknowledged.

- *Email address: stepan@valinux.physik.uni-halle.de
- ¹I.L. Grigorov, M.R. Fitzsimmons, I-Liang Siu, and J. C Walker, *Phys. Rev. Lett.* **82**, 5309 (1999); S.M. Jordan, R. Schad, A.M. Keen, M. Bischoff, D.S. Schmool, and H. van Kempen, *Phys. Rev. B* **59**, 7350 (1999); C. Xu, W.S. Oh, G. Liu, D.Y. Kim, and D.W. Goodman, *J. Vac. Sci. Technol. A* **15**, 303 (1997).
 - ²J.M. Zuo, M. O'Keeffe, P. Rez, and J.C.H. Spence, *Phys. Rev. Lett.* **78**, 4777 (1997).
 - ³J.-M. Gillet and P. Cortona, *Phys. Rev. B* **60**, 8569 (1999).
 - ⁴P. Jonnard, F. Vergand, C. Bonnelle, E. Orgaz, and M. Gupta, *Phys. Rev. B* **57**, 12 111 (1998).
 - ⁵S.A. Canney, V.A. Sashin, M.J. Ford, and A.S. Kheifets, *J. Phys.: Condens. Matter* **11**, 7507 (1999).
 - ⁶U. Schönberger and F. Aryasetiawan, *Phys. Rev. B* **52**, 8788 (1995).
 - ⁷V.S. Stepanyuk, A.A. Grigorenko, O.V. Farberovich, and A.A. Katsnelson, *Sov. Phys. Solid State* **31**, 2010 (1989); A.A. Katsnelson, V.S. Stepanyuk, A. Szasz, O.V. Farberovich. *Computational Methods in Condensed Matter: Electronic Structure* (AIP, Woodbury, NY, 1992).
 - ⁸B.M. Klein, W.E. Pickett, L.L. Boyer, and R. Zeller, *Phys. Rev. B* **35**, 5802 (1987).
 - ⁹A. De Vita, M.J. Gillan, J.S. Lin, M.C. Payne, I. Stich, and L.J. Clarke, *Phys. Rev. B* **46**, 12 964 (1992).
 - ¹⁰P. Cortona and A.V. Monteleone, *J. Phys.: Condens. Matter* **8**, 8983 (1996).
 - ¹¹M.J. Mehl, R.E. Cohen, and H. Krakauer, *J. Geophys. Res., [Atmos.]* **93**, 8009 (1988).
 - ¹²K. Doll, M. Dolg, and H. Stoll, *Phys. Rev. B* **54**, 13 529 (1996).
 - ¹³K.J. Chang and M.L. Cohen, *Phys. Rev. B* **30**, 4774 (1984).
 - ¹⁴G. Timmer and G. Borstel, *Phys. Rev. B* **43**, 5098 (1991).
 - ¹⁵O. Schütt, P. Pavone, W. Windl, K. Karch, and D. Strauch, *Phys. Rev. B* **50**, 3746 (1994).
 - ¹⁶J. Yamashita and S. Asano, *J. Phys. Soc. Jpn.* **28**, 1143 (1970).
 - ¹⁷O.E. Taurian, M. Springborg, and N.E. Christensen, *Solid State Commun.* **55**, 351 (1985).
 - ¹⁸S. Pantelides, D.J. Mickisch, and A.B. Kunz, *Phys. Rev. B* **10**, 5203 (1974).
 - ¹⁹G. Bihlmayer and S. Blügel (private communications).
 - ²⁰A. Strachan, T. Cagin, and W.A. Goddard, Jr., *Phys. Rev. B* **60**, 15 084 (1999).
 - ²¹Y. Yan, M.F. Chisholm, D. Duscher, A. Maiti, S.J. Pennycook, and S.T. Pantelides, *Phys. Rev. Lett.* **17**, 3675 (1998).
 - ²²R. Souda, Y. Hwang, T. Aizava, W. Hayami, K. Oyoshi, S. Hishita, *Surf. Sci.* **387**, 136 (1997).
 - ²³M. Asato, A. Settels, T. Hoshino, T. Asada, S. Blügel, R. Zeller, and P.H. Dederichs, *Phys. Rev. B* **60**, 5202 (1999).
 - ²⁴N. Papanikolaou, R. Zeller, P.H. Dederichs, and N. Stefanou, *Phys. Rev. B* **55**, 4157 (1997).
 - ²⁵J.P. Perdew, in *Electronic Structure of Solids '91*, edited by P. Ziesche and H. Eschrig (Academie Verlag, Berlin, 1991), p. 11.
 - ²⁶B. Drittler, M. Weinert, R. Zeller, and P.H. Dederichs, *Solid State Commun.* **79**, 31 (1991).
 - ²⁷N. Stefanou, H. Akai, and R. Zeller, *Comput. Phys. Commun.* **60**, 231 (1990); N. Stefanou, and R. Zeller, *J. Phys.: Condens. Matter* **3**, 7599 (1991).
 - ²⁸F. Birch, *J. Geophys. Res. B* **83**, 1257 (1978).
 - ²⁹M.L. Sangster, G. Peckham, and D.H. Sanderson, *J. Phys. C* **3**, 1026 (1970).
 - ³⁰D.H. Chung and G. Simmons, *J. Geophys. Res.* **74**, 2133 (1969).
 - ³¹A.J. Cohen and R.G. Gordon, *Phys. Rev. B* **14**, 4593 (1976).
 - ³²H.G. Drickamer, R.W. Lynch, R.L. Clendenen, and E.A. Perez-Albuerne *Solid State Phys.* **19**, 135 (1966).
 - ³³R.W.G. Wyckoff, *Crystal Structure* (Wiley, New York, 1965), Vol. 1.
 - ³⁴W. Pies and A. Weiss, in *Numerical Data and Functional Relationships in Science and Technology*, Landolt-Börnstein, edited by K.-H. Hellwege and A.M. Hellwege, New Series, Group III, Vol. 7, Pt. bl (Springer Verlag, Berlin, 1975), p. 26.
 - ³⁵M.J.L. Sangster and A.M. Stoneham, *Philos. Mag. B* **43**, 597 (1981).
 - ³⁶O.L. Anderson and P. Andreatch, *J. Am. Ceram. Soc.* **49**, 404 (1966).